# Investigation of Reinforced Sic Particles Percentage on Machining Force of Metal Matrix Composite

Morteza Fathipour[1], Pouya Zoghipour[2], Javad Tarighi[3] & Reza Yousefi[4]

[1] Department of Mechanical Engineering, University of Tehran, Tehran, Iran

[2] Faculty of Mechanical Engineering, Babol Noshirvani University of Technology, Mazandaran, Iran

[3] Department of Mechanical Engineering of Agriculture Machinery, University of Tabriz, Iran

[4] Educational Workshop Center, Mechanical Engineering Department, Sharif University of Technology, Tehran, Iran

Correspondence: Mortaza Fathipour, Department of Mechanical Engineering, University of Tehran, Tehran, Iran. E-mail: mfathipour@ut.ac.ir

## Abstract

In this study two-dimensional finite element models of Al/SiC metal matrix composites (MMC) by using of ABAQUS Explicit software are investigated. Chip formations and machining forces for three types of MMC with 5, 15 and 20% of SiC reinforcement particles were studied and compared with experimental data. The resulted chips in simulation and the generated chips in experiments have both continuous and saw tooth in appearance. On the other hand, the variation of the cutting forces with the cutting time in simulation and experiment have fluctuating diagram. This is due to the interaction between cutting tool and SiC particles during chip formation. ABAQUS explicit software was used for simulation; it was found that there are good agreements with simulation and experimental data.

**Keywords:** chip formation, simulation, metal matrix composite, ABAQUS

## 1. Introduction

Metal Matrix Composites (MMCs) have replaced common materials in many applications, especially in aerospace and automotive industries, because of their superior properties such as high specific strength, high wear resistance, high thermal conductivity and low coefficient of thermal expansion. Nowadays, MMCs usually are produced close to the final dimension in different methods but in most engineering applications, machining is necessary to get the final dimensions. The existence of hard particles or fibers in soft metal matrix influences on machinability of MMCs.

Many experiment studies have done on machining mechanism of particle - reinforced metal matrix composites (MMC). Kanan and Kishawy (2008) have studied tool wear, surface integrity and chip formation under dry and wet cutting conditions. They illustrated subsurface damage after machining and pit holes after particle debonding in machined surface and also the influence of cutting fluid on chip formation.

Manna and Bhattacharayya (2003) have studied chip formation mechanism of Al/SiC$_p$ experimentally. They have managed to generate two types of chip formation for coarser reinforced composite and finer reinforced composite.

One of the best analytical studies on prediction of metal cutting forces is done by Paramanik et al. (2006). They divided force generation mechanism to three parts: a) the chip formation force, b) the ploughing force and c) the particle fracture force. The chip formation force was obtained by merchant's theory but those due to matrix ploughing and deformation and fracture mechanism of particle were formulated with slip line theory of plasticity and the Grifith theory of fracture, respectively. They developed a model that has excellent agreement with the experimental results. Their prediction revealed that the cutting forces due to chip formation are higher than those due to ploughing and particle fractures. There are only few researches performed in machining of metal matrix composite by finite element software, because of its difficulties and complexity. Monaghan and Brazil (1998) modeled machining of Aluminum matrix composite by FORGE2 software with Elasto-Visco-plastic FEA code

in advance and then micromechanical sub modeling was modeled by ANSYS software. Although, their studies include some commendable cases such as study on non-uniform matrix flow, particle-matrix interface failure, and residual stress in MMC due to thermal cycling and tool pressure, it wasn't able to illustrate tool-particle interaction due to machining, matrix debonding and pit holes of machined surface. Ramesh et al. (2001) studied diamond turning mechanism of $Al6061/SiC_p$, they presented four models to describe the tool interface with Al-SiC work-pieces; (a): Tool facing SiC element, (b): Tool facing Aluminum matrix, (c): Tool ploughing SiC element, and (d): Tool ploughing Aluminum matrix. Their models were not suitable for describing the machining of composite material because in each model tool faces pure the material. For example when tool faces SiC elements in case (a), the tool contains no aluminum material and also their model was unable to illustrate chip formation Pramanik et al. (2007) studied machining behavior of metal matrix composite by ANSYS/LS-DYNA software. They illustrated tool-particle interaction during orthogonal cutting and obtained stresses during machining. They modeled a pore matrix that circle particles were adjusted in that pore area and the interface of matrix and particles ties them together. Their model illustrated the actual function of MM composites material during machining process but they didn't study machining parameters which affect cutting forces. Dandekar and Shin (2009) have studied subsurface damage and particle matrix debonding in MMC with 20% SiCp and cohesive zone element implemented in the particle-matrix interface. They simulated 3-D nose turning model in Third Wave Advent Edge software by using random particle dispersion algorithm, they also studied stress and temperature distribution on the work-piece during machining. For 2-D simulation of MMC cutting they used ABAQUS/explicit. It is very expensive and complicated task to study the machining behavior of MMCs. Therefore, a machining model that can illustrate their machining behavior would be so useful. Nowadays simulation of most processes such as monolithic metal cutting has been facilitated by the advances in finite element software. While in simulation of machining metal matrix composite due to existence of more than two different materials, simultaneously, the model is somehow complicated. As the model in MMC simulation must illustrate the interaction between tool and particle during chip formation, the tool wear is actually very important factor during machining of MMC (Pramanik, Zhang, & Arsecularatne, 2007; Dandekar & Shin, 2009).

## 2. Machining Parameters Effects on Simulation

Effective parameters on MMC machining forces have shown in Figure 1. Any change in the machining parameters results a change in machining forces. In this study, the effect of cutting speed, feed rate and depth of cut on the machining forces have been investigated in machining of MMC with three different percentages (5, 15 and 20%) of SiC reinforcement particles.
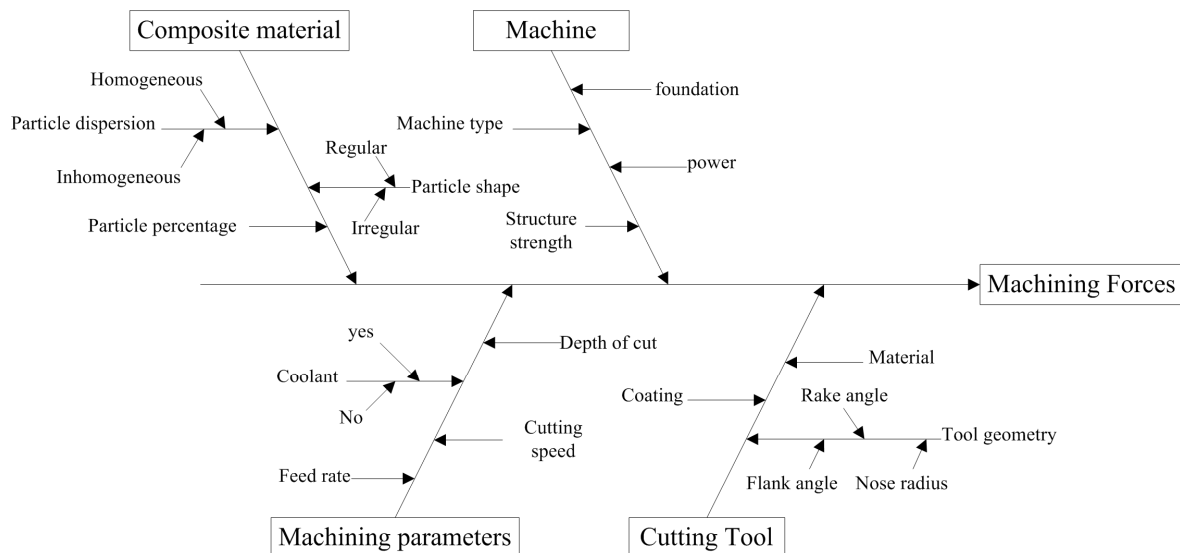


Figure 1. Fish bon for showing the influence of machining parameters on cutting force

## 3. Two-Dimensional Modeling

ABAQUS/Explicit finite element software was employed for MMC machining simulation. Two-dimensional finite element model using Lagrangian formulation was used to develop plane-strain model. Unlike monolithic machining simulation, workpiece is consisted of two parts; matrix and SiC particle. Each of them was modeled

separately and then assembled together. Particle-matrix interfaces were tied together after assembling. Therefore, the initial displacement in the interface will be equal for both the matrix and particles as shown in Figure 2. The particles with 20 μm of diameter were distributed homogenously in the matrix. The boundary conditions and the workpiece size have been shown in Figure 3. The cutting tool treats as a rigid body moving according to the cutting direction and the other degrees of freedom are restricted.
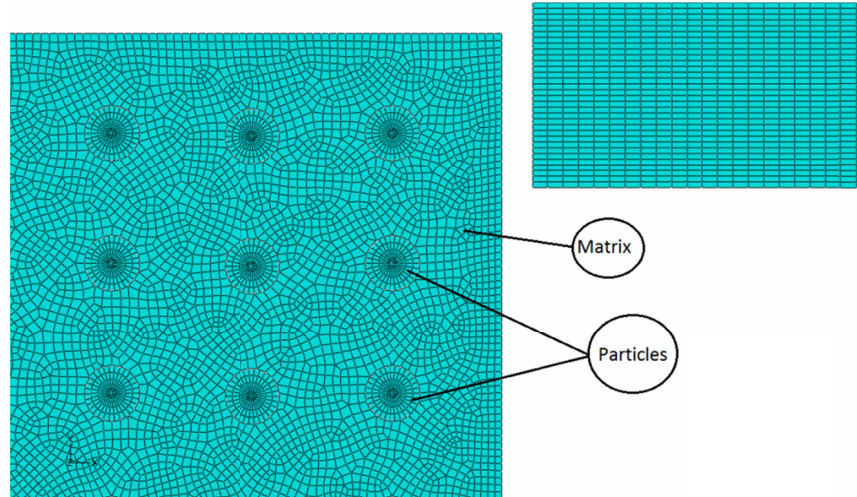
Figure 2. Work piece and the cutting tool assembled model for MMC machining simulation
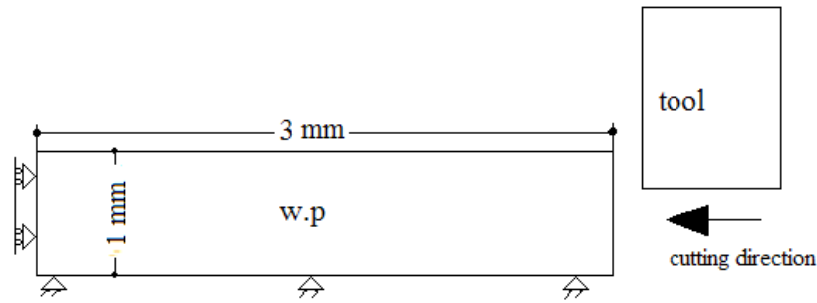
Figure 3. The boundary conditions and the workpiece dimension in simulation

## 4. Material Properties

In this study, Johnson-Cook plasticity model was utilized Aluminum matrix plasticity behavior. In this model flow stress is dependent on strain ($\varepsilon^{pl}$), strain rate ($\dot{\varepsilon}^{pl}$), and homologous temperature ($T^*$). The following Johnson-Cook constitutive equation is used:

$$\sigma_y = \left[ A + B\left(\varepsilon^{pl}\right)^n \right] . \left[ 1 + C.ln\left( \frac{\dot{\varepsilon}^{pl}}{\dot{\varepsilon}_0} \right) \right] . \left[ 1 - \left(T^*\right)^m \right] \tag{1}$$

$$T^* = \frac{T - T_{room}}{T_{melt} - T_{room}} \tag{2}$$

Where A, B, C, m, are material constants and n is the strain hardening index. The Johnson-Cook dynamic failure model is based on the value of the equivalent plastic strain at element integration points; failure is assumed to occur when the damage parameter exceeds 1. The damage parameter, ω, is defined as:

$$\omega = \sum \frac{\Delta \overline{\varepsilon}^{pl}}{\overline{\varepsilon}_f^{pl}} \tag{3}$$

Where $\Delta\bar{\varepsilon}^{pl}$ is an increment of the equivalent plastic strain, $\bar{\varepsilon}_f^{pl}$ is the strain at failure, and the summation is performed over all increments in the analysis. The strain at failure, $\bar{\varepsilon}_f^{pl}$ is assumed to be dependent on a non-dimensional plastic strain rate, $\dot{\varepsilon}^{pl}/\dot{\varepsilon}_0$; a dimensionless pressure-deviatory stress ratio, p/q (where p is the pressure stress and q is the Misses stress); and the non-dimensional temperature, T*, defined earlier in the Johnson-Cook hardening model. The dependencies are assumed to be separable and are of the form:

$$\varepsilon_f = \left[ d_1 + d_2\ exp\left( d_3\ \frac{p}{q} \right) \right]\left[ 1 + d_4\ ln\left( \frac{\dot{\varepsilon}^{pl}}{\dot{\varepsilon}_0} \right) \right] \times \left[ 1 + d_5\left( \frac{T - T_{room}}{T_{melt} - T_{room}} \right) \right] \tag{4}$$

Where $d_1$-$d_5$ are failure parameters measured at or below the transition temperature, $T_{room}$, and $\dot{\varepsilon}_0$ is the reference strain rate (ABAQUS user manual v6.10).

The particle flow stress was assumed to be isotropic elastic material following the generalized Hook's law, particle fracture omitted for simplicity and particle debonding occurred due to matrix failure around it. Material properties for matrix, particle and tool are given in Table 1.

Surface to surface contact and Coulomb friction model was used for contact during machining.

$$\tau = \mu.P \tag{5}$$

Where μ is the friction coefficient, P contact pressure, we assumed that friction coefficient during machining is 0.45, were based on the study reported in Dandekar and Shin (2009).

Table 1. Material properties for Matrix, Particle and Cutting Tool

| Al 1100 | Mat. Johnson Cook | | | | | | |
|---------|-------------------|---|---|---|---|---|---|
| **(Matrix)** | $\rho$(kg/m-3) | E(GPa) | | $\upsilon$ | | | |
| | 2700 | 70 | | 0.27 | | | |
| | A(MPa) | B(MPa) | n | c | m | $T_m$(K) | $T_0$(K) |
| | 148 | 361 | 0.183 | 0.001 | 0.859 | 1220 | 298 |
| | $d_1$ | $d_2$ | | $d_3$ | $d_4$ | $d_5$ | |
| | 0.071 | 1.248 | | -1.142 | 0.147 | 0.1 | |
| **Particle** | Mat. Elastic | | | | | | |
| **(SiC)** | $\rho$(kg/m-3) | | E(GPa) | | $\upsilon$ | | |
| | 3200 | | 400 | | 0.17 | | |
| | Mat. Elastic | | | | | | |
| **Tool** | $\rho$(kg/m-3) | | E(GPa) | | $\upsilon$ | | |
| | 1500 | | 800 | | 0.2 | | |

## 5. Research System and Test Conditions

### 5.1 Fabrication Method

SiC particles powder with mesh 800 and average size of 18-20 μm were utilized as reinforcing particles. Preparation of Al/SiC composites needs two manufacturing steps. First, aluminum with average particle size of 63 μm and SiC powder was mixed for 150 minutes in a rotary mixer and the mixture was pressed into aluminum cans with a pressure of 70 tons. Subsequently, the billets were preheated for 180 minutes at 500°C under argon environment and extruded with an extrusion ratio of 15.

### 5.2 Test Conditions

The bar-shape samples of 13 mm in diameter and 135 mm in length were machined by titanium carbide (K10) insert tools which are generally recommended for machining of metal matrix composites. The tool rake angle is 5 degree, the clearance angle is 5 degree and the nose Radius is 60 μm. The turning process carried out as dry machining for machining 95 mm in length of the composite bars for each test. The details of the experimental conditions are summarized in Table 2. The experimental set up is illustrated in Figure 4 schematically.

Table 2. Test conditions

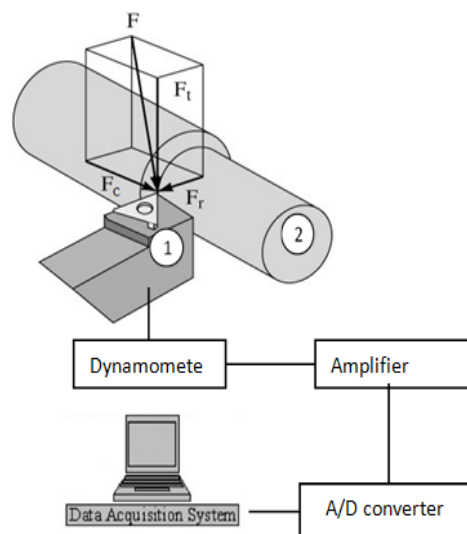| Machine | TN50BR Lathe Machine of Machine Sazi Tabriz Co. |
|---|---|
| Cutting speed (m/min) | 20, 30, 50, 60 and 80 |
| Feed rate (mm/rev) | 0.08, 0.16, 0.24 and 0.32 |
| Depth of cut (mm) | 0.4, 0.8 and 1.2 |
| Percentage of SiC particles | 5, 15 & 20 |
| Cutting Condition | Dry |
| Cutting length (mm) | 95 |



Figure 4. Schematic view of setup

(1) Cutting tool (2) Work piece

## 6. Result and Discussion

*6.1 Chip Formation*

In this study the chip formation and machining forces for three types of MMC with 5%, 15% and 20% were studied. The chips resulted from simulations are continuous or semi continuous depending upon the cutting conditions.

Chip separation is normally performed along the interface of the matrix and particles by deleting elements. Figures 5 to 7 show the form of chip formation during machining for three types of MMC with 5%, 15% and 20% of SiC particles. Comparing the experimental with simulation results shows that the saw-tooth shapes are common features of the chip form produces in MMC machining (Figures 5 to 7 with Figure 8).
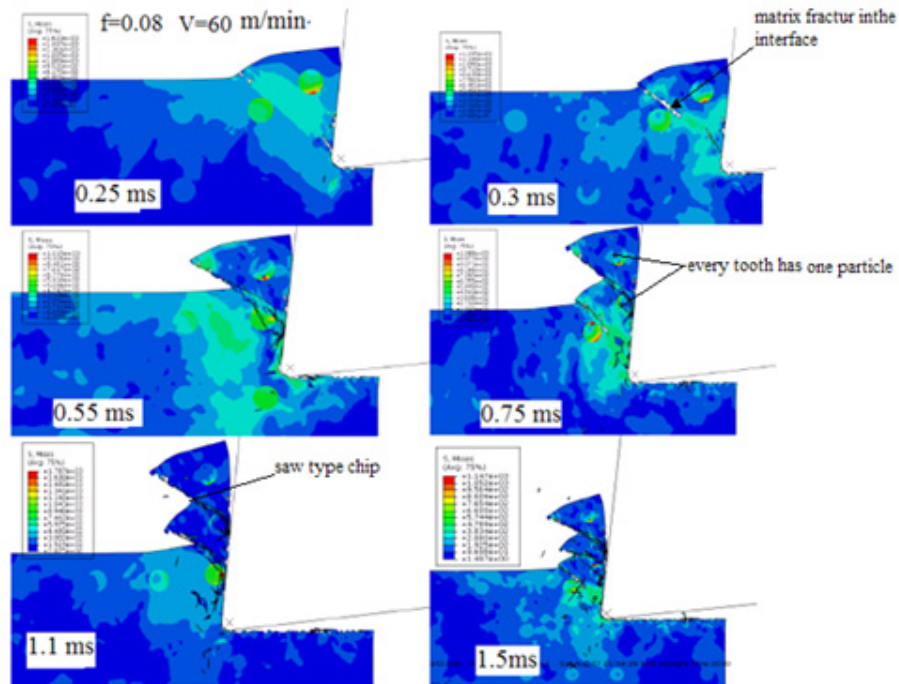
Figure 5. Chip formation in machining of MMC with 5% of SiC particle
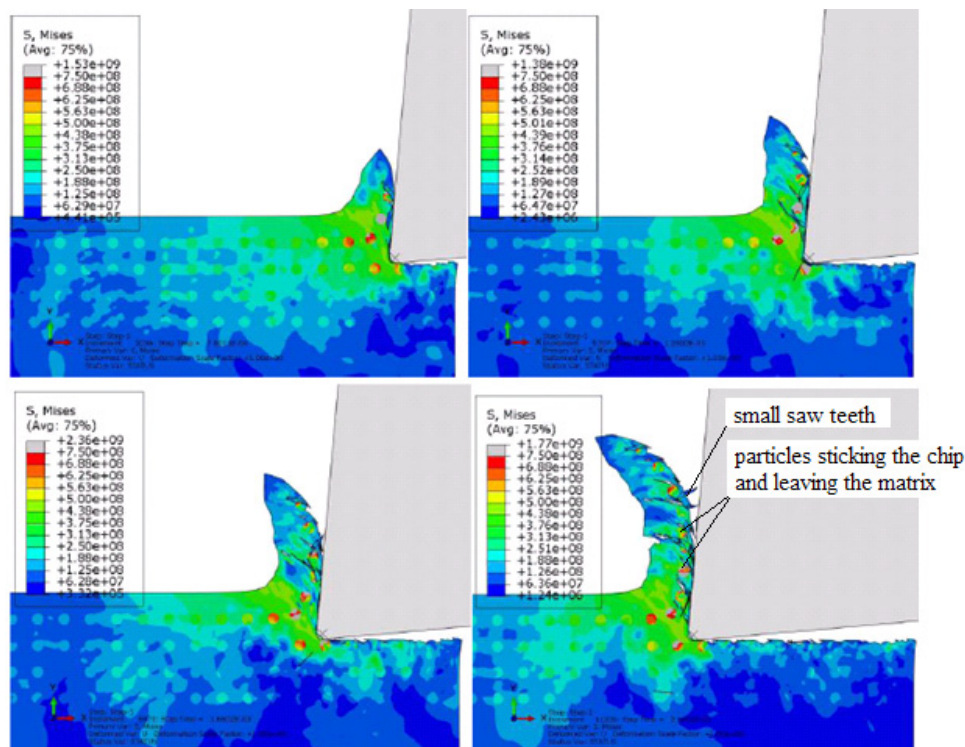(Cutting speed = 60 m/min, Feed rate = 0.08 mm/rev and Depth of cut = 0.8 mm)



Figure 6. Chip formation in machining of MMC with 15% of SiC particle
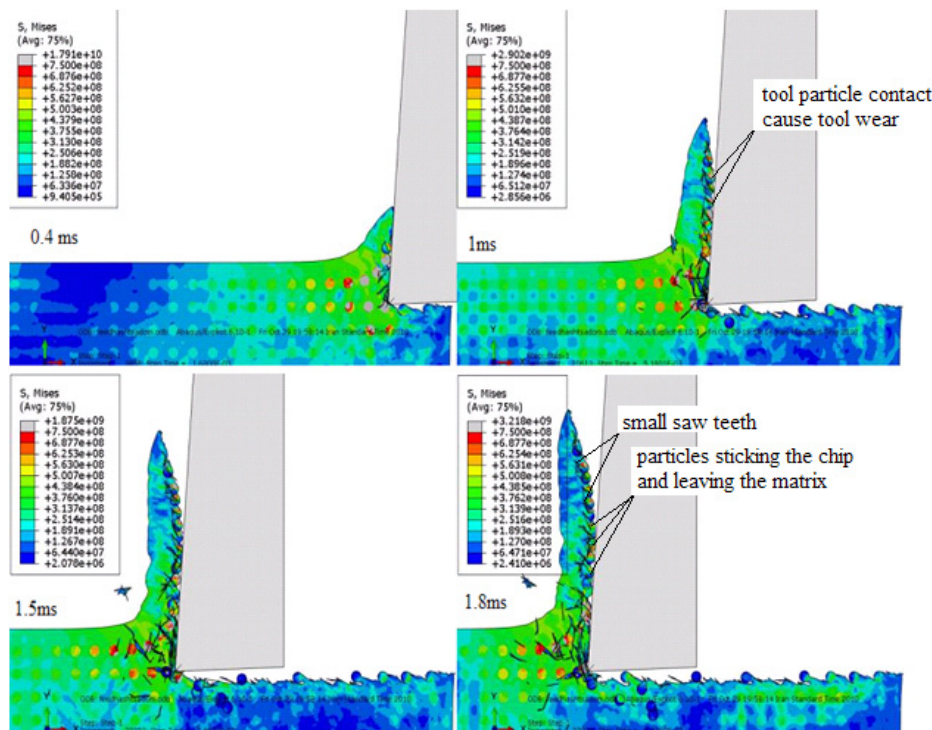(Cutting speed = 60 m/min, Feed rate = 0.08 mm/rev and Depth of cut = 0.8 mm)

Figure 7. Chip formation in machining of MMC with 20% of SiC particle

(Cutting speed = 60 m/min, Feed rate = 0.08 mm/rev and Depth of cut = 0.8 mm)

Figure 8 illustrates the back side of the chips generated in the experimental at specific machining conditions, cutting speed = 60 m/min, feed rate = 0.08 mm/rev and depth of cut = 0.8 mm.
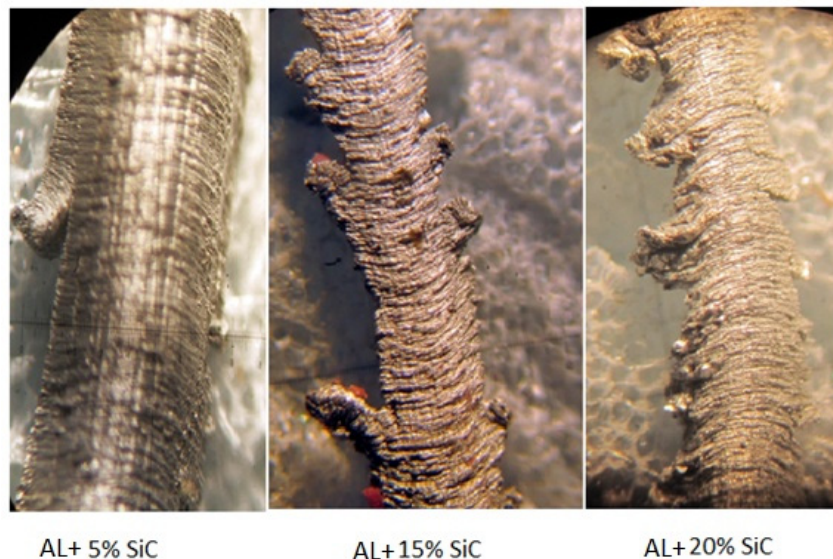


Figure 8. Chip configuration in machining of MMCs with 5%, 15% and 20% of SiC particle

(Cutting speed = 60 m/min, Feed rate = 0.08 mm/rev and Depth of cut = 0.8 mm)

As shown in Figure 8 increasing the percentage of SiC in the work material causes more and compressed lamellae structure on the back of the chips ribbons. The reason of this phenomenon is due to the SiC particles that play as the obstacles on the way of plastic deformations of the aluminum matrix. When the stream line of the plastic deformations of the pure aluminum matrix reaches to these barriers (SiC particles), they attempt to run

over them but they could not pass over them. Therefore, they change to lamella features. The more percentage of SiC generates the more lamellae feature on the back of the chips.

When cutting parameters such as feed rate, depth of cut and velocity kept constant, by increasing the percentage of SiC particles in the matrix the amount of the SiC particle that sticks the chip and leave the matrix are increased. Increasing particles in the chip exceed tool-particle contacts that raises the tool wear.

### 6.2 Machining Forces

The forces diagrams obtained from simulation have many fluctuations as shown in Figure 9. Since the cutting force which is needed for debonding the SiC particles is higher than the force which is needed for shearing the pure aluminum matrix; so the cutting force rises at debonding process and falls at cutting or shearing conditions of the matrix. On the other hand, there is a random dispersion of SiC particles in the matrix; so the resulted fluctuations in the experimental cutting force diagram have also a random feature. These fluctuations in force diagrams increases by the increase of the SiC particles percentage in the matrix. The fluctuations are observed in the cutting forces diagram obtained from simulation too, as shown in Figure 10. The fluctuating in simulation force diagram is more regular than the fluctuating in experimental force diagram. This is due to the regular and orderly dispersion of SiC throughout the matrix in the simulation model while the SiC has a random distribution in real metal matrix composites.

For comparison of the experimental and simulation results; the average values of these diagrams have been used.
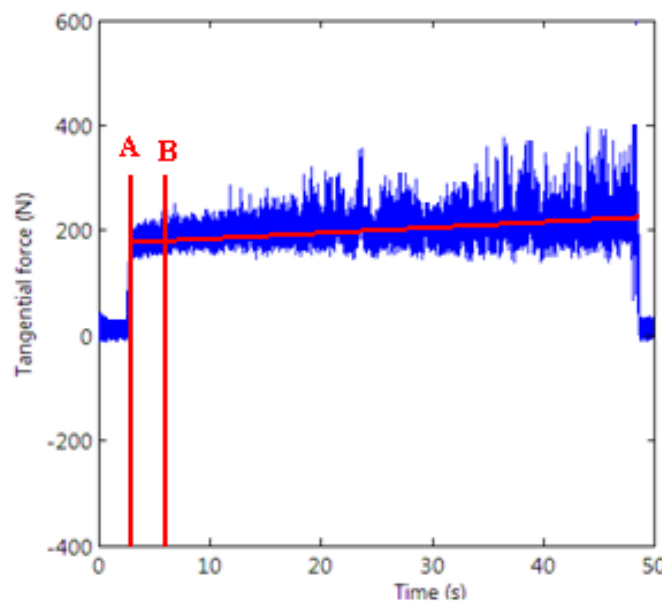


Figure 9. Fluctuations in experimental machining forces diagram

(Cutting speed = 60 m/min, Feed rate = 0.08 mm/rev and Depth of cut = 0.8 mm)

According to Figure 9 the average amount of the force diagram increases during the machining time. This is because of tool wear that occurs in this period of time. So the average value of machining forces in the primary shear region i.e. AB which is equal to 3 seconds of machining time is used as criteria for comparison. The tool wear in the first 3 seconds of machining time is negligible and the cutting force is very near to the simulation conditions, because in the simulation model it is supposed that the tool edge is very sharp and the tool wear does not occur during the machining time.
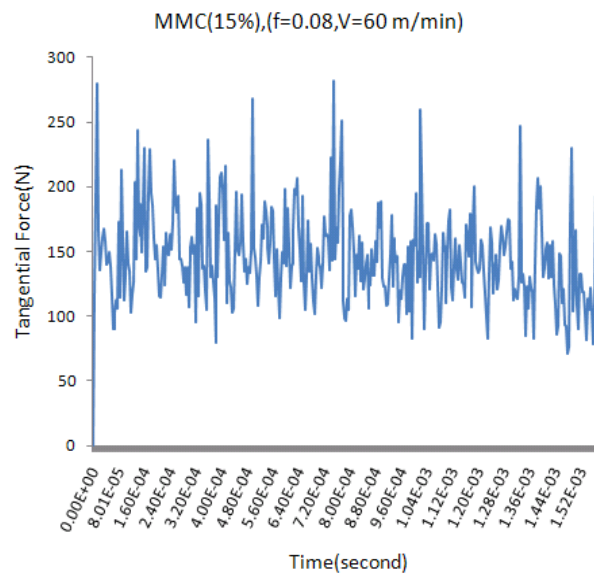
Figure 10. Fluctuations in simulation machining forces diagram
(Cutting speed = 60 m/min, Feed rate = 0.08 mm/rev and Depth of cut = 0.8 mm)

### 6.2.1 Experimental Results

#### 6.2.1.1 Machining Force and Cutting Speed

The variation of the machining force with cutting speed is indicated in Figure 11. As shown in this figure, tangential force decreases with the increase of cutting speed. The reason of this reduction could be explained by the reduction of built-up edge (BUE) thickness with the increase of cutting speed. According to Manna et al. in the machining of Al/SiC MMC material, the chance of formation of BUE is higher at lower cutting speed, feed and higher depth of cut (Dandekar & Shin, 2009). The results of BUE formation in this experiment are also shown in Figure 12. The thickness of BUE decreases with the increase of cutting speed. For example, in cutting speed of 80 m/min the thickness of BUE reaches to the lowest amount i.e. 0.11 mm in sample with 20 Wt% of SiC.

In addition to the reduction of BUE thickness, the other factor which reduces the tangential cutting forces is the increase in shear angle with increasing the cutting speed. The larger shear angle causes lower shear forces in the primary shear zone. Third reason for reduction of cutting forces can be the thermal softening of the aluminum matrix, which occurs with increasing cutting temperature. The amount of heat generated in machining of powder extruded Al-SiC MMC is more than the heat generated in non-composite material.
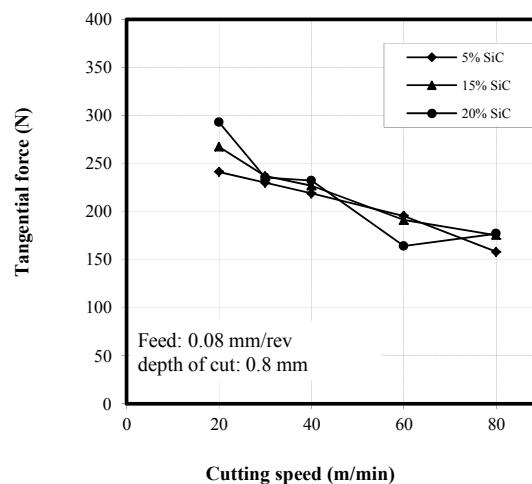


Figure 11. Tangential force versus cutting speed
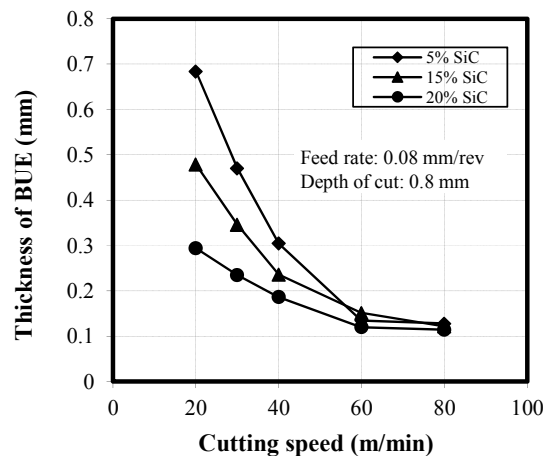(Cutting speed = 60 m/min, Feed rate = 0.08 mm/rev, Depth of cut = 0.8 mm)

Figure 12. Variation of BUE thickness with cutting speed

(Cutting speed = 60 m/min, Feed rate = 0.08 mm/rev, Depth of cut = 0.8 mm)

6.2.1.2 Machining Force and Feed Rate

Variation of tangential machining force with feed rate is shown in Figure 13. The tangential force increases at higher feed rates in all samples. Comparing Figure 11 with Figure 13 indicates that the cutting speed is more effective on tangential force than the feed rate.
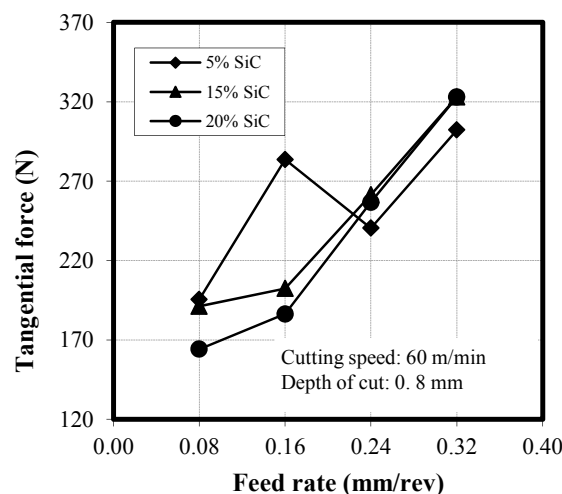


Figure 13. Tangential force versus feed rate

(Cutting speed = 60 m/min, Feed rate = 0.08 mm/rev and Depth of cut = 0.8 mm)

6.2.2 Simulation Results

The comparison of the tangential cutting force with the cutting speed for three types of metal matrix composites are illustrated in Figure 14. It shows that shows that with increasing in the cutting speed the tangential forces decrease as was observed and discussed in the experimental results. The difference between experimental and simulation results may be due to the formation of BUE that existed in the experiment conditions and supposed no to be formed in simulation conditions.

The variation of the cutting force with the feed rate in simulation results is shown in Figure 15. For three types of metal matrix composites the tangential force increase by increasing the feed rate. There is a maximum deviation of 15% between experimental and simulation results. This is because of some assumptions that have been considered for simplifying the simulation conditions.
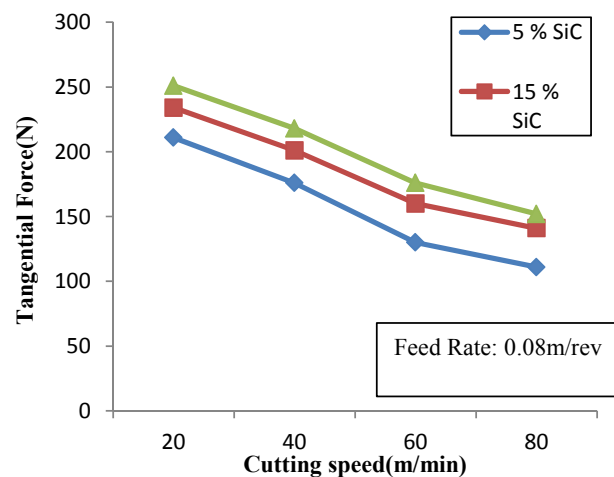
Figure 14. Tangential force versus cutting speed obtained from simulation
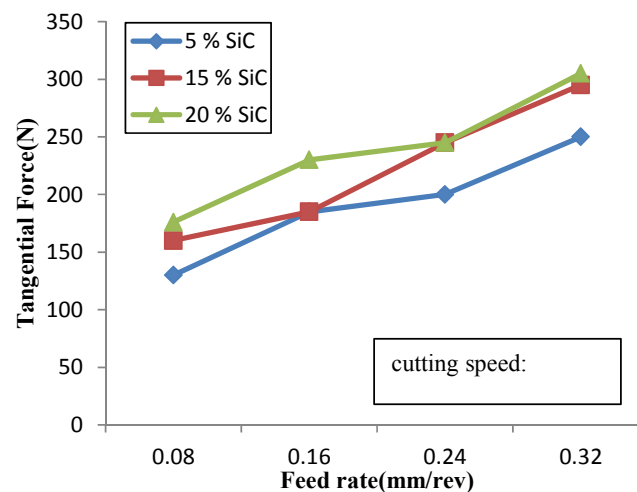(Cutting speed = 60 m/min, Feed rate = 0.08 mm/rev and Depth of cut = 0.8 mm)



Figure 15. Tangential force versus feed rate obtained from simulation
(Cutting speed = 60 m/min, Feed rate = 0.08 mm/rev and Depth of cut = 0.8 mm)

## 7. Conclusions

2-D finite element model was used for orthogonal machining simulation of metal matrix composite with different percent (5%, 15%, 20%) of SiC reinforcement particle. Chip formation and machining forces are investigated in this study. Good agreement was found between obtained results from this study and the experimental results. The followings may be concluded:

(a) Investigated forces diagram from simulations have many fluctuations during machining. These fluctuations also have been seen in the experimental forces diagram. However, in the simulation case these fluctuations are more regular because the SiC particles in the simulation model have a geometric distribution while these particles have a random distribution in the aluminum matrix.

(b) The amounts of cutting forces obtained from experiments have good agreement with results obtained from simulation. There is only a maximum deviation of 15% between experimental and simulation results. This is because of some assumptions that have been considered for simplifying the simulation conditions.

**References**

ABAQUS user manual v6.10.

Dandekar, C. R., & Shin, Y. C. (2009). Multi-step 3-D finite element modeling of subsurface damage in machining particulate reinforced metal matrix composites. *Composites Part A: Applied Science and Manufacturing, 40*(8), 1231-1239. http://dx.doi.org/10.1016/j.compositesa.2009.05.017

Kannan, S., & Kishawy, H. A. (2008). Tribological aspects of machining aluminium metal matrix composites. *Journal of Materials Processing Technology, 198*(1-3), 399-406. http://dx.doi.org/10.1016/j.jmatprotec.2007.07.021

Manna, A., & Bhattacharayya, B. (2003). A study on machinability of Al/SiC-MMC. *Journal of Materials Processing Technology, 140*(1-3), 711-716. http://dx.doi.org/10.1016/S0924-0136(03)00905-1

Monaghan, J., & Brazil, D. (1998). Modelling the flow processes of a particle reinforced metal matrix composite during machining. *Composites Part A: Applied Science and Manufacturing, 29*(1-2), 87-99. http://dx.doi.org/10.1016/S1359-835X(97)00047-X

Pramanik, A., Zhang, L. C., & Arsecularatne, J. A. (2006). Prediction of cutting forces in machining of metal matrix composites. *International Journal of Machine Tools and Manufacture, 46*(14), 1795-1803. http://dx.doi.org/10.1016/j.ijmachtools.2005.11.012

Pramanik, A., Zhang, L. C., & Arsecularatne, J. A. (2007). An FEM investigation into the behavior of metal matrix composites: tool-particle interaction during orthogonal cutting. *International Journal of Machine Tools and Manufacture, 47*(10), 1497-1506. http://dx.doi.org/10.1016/j.ijmachtools.2006.12.004

Ramesh, M. V., Chan, K. C., Lee, W. B., & Cheung, C. F. (2001). Finite-element analysis of diamond turning of aluminium matrix composites. *Composites science and technology, 61*(10), 1449-1456. http://dx.doi.org/10.1016/S0266-3538(01)00047-1